Metastable phase formation in the Zr-Al binary system induced by mechanical alloying

H. J. Fecht, G. Han, Z. Fu, and W. L. Johnson
W. M. Keck Laboratory of Engineering Materials, California Institute of Technology, Pasadena, California 91125

(Received 23 June 1989; accepted for publication 5 October 1989)

We have studied the sequence of phase transformations induced in the Zr-Al binary system by mechanical alloying of mixed Zr and Al powders. The structure of these materials has been studied by transmission electron microscopy and by x-ray diffraction measurements. Three different metastable phases have been found experimentally with variation of the initial composition x_{Al}: (1) a nanocrystalline supersaturated solid solution of α-Zr for $x_{Al} \leqslant 0.15$, (2) an amorphous phase for $0.15 < x_{Al} \leqslant 0.4$, and (3) a metastable face-centered-cubic phase for $x_{Al} = 0.5$ with a grain size of 4 nm. The crystallization reaction of the amorphous phase was monitored by differential scanning calorimetry, and the kinetics of the reaction have been examined as well. A possible explanation based on thermodynamic arguments is given for the defect-driven vitrification of the crystalline Zr phase.

I. INTRODUCTION

Over the last several years, a considerable amount of work has been performed on amorphization induced by mechanical alloying (MA) of binary systems (for a review see Ref. 1). It is now known that amorphous phases can be synthesized by MA of either intermetallic compound powders or a mixture of elemental metal powders. For mixed elemental powders, Yermakov, Yurchikov, and Barinov[2] have hypothesized that MA induces amorphization by a process of formation of local melts followed by rapid solidification of these melts to the amorphous phase. In contrast, Schwarz, Petrich, and Saw[3] and Hellstern and Schultz[4] have argued that amorphization by MA results from a solid-state reaction between ultrafine crystalline particles with fresh surfaces created by MA of appropriate duration. In the case of amorphization of an intermetallic compound, Koch *et al.*[5] suggested that the following mechanism might be responsible: the severe plastic deformation provided by MA generates lattice defects (point defects, dislocations, etc.) which cause the free energy of the crystalline phase to rise above that of the amorphous phase, resulting in vitrification of the compound phase. More recently, Johnson[1] suggested an elastic instability as a mechanism for the crystal-to-amorphous phase transformation in analogy to irradiation-induced amorphization. A large (about 50%) elastic softening and dilation strain (about 3%) due to disordering that precedes the onset of amorphization of the intermetallic compound Zr_3Al during room-temperature bombardment with 1.0-MeV Kr^+ provides experimental support for this hypothesis.[6] However, despite the numerous experiments using MA, the exact mechanism of how amorphization takes place at the microstructural level has not been determined.

The present study was designed to investigate the principles underlying the crystal-to-glass phase transition in the Zr-Al binary system by MA of mixed Zr and Al elemental powders. The sequence of phase transformations for the Zr-Al binary system is described and a new mechanism for the vitrification process is given.

II. EXPERIMENTAL METHOD

Mechanical alloying of a mixture of pure Zr powder (99.5%, -80 mesh) and pure Al powder (99.95%, -40 mesh) was carried out in a laboratory ball mill (Spex 8000) using a hardened steel vial and tungsten carbide balls. The weight of the mixed powder sample for each composition was about 10 g and the ratio of ball weight to powder weight was 4:1. To minimize oxidation the loaded vials were always sealed under a dry argon atmosphere at an Ar overpressure of 3 atm. The vial temperature during MA was held constant by air cooling. The ball milling process was periodically interrupted to remove sample portions and the agglomeration of powder on the vial and balls was reduced or eliminated by mechanical scraping. The overall powder compositions were varied between 0 and 70 at. % Al. In all cases, wet chemical analysis and EDAX analysis indicated impurity levels of less than 300 ppm oxygen and 1 at. % iron.

The ball-milled powders were analyzed by x-ray diffraction (XRD), scanning electron microscopy (SEM), transmission electron microscopy (TEM), and differential scanning calorimetry (DSC). X-ray scans were carried out on a Norelco Philips powder diffractometer in step scanning mode using Cu$K\alpha$ radiation ($\lambda = 0.15418$ nm) filtered with nickel foil. A Philips EM430 equipped with EDX detector and STEM unit was used for TEM experiments. Ultrathin sections (20–50 nm) of powder particles were prepared with a diamond knife using an ultramicrotome. The sections were retrieved from water onto Cu grids coated with a holey-carbon substrate.

A Perkin–Elmer DSC-4 was employed for thermal analysis including the measurement of heat capacity c_p and excess enthalpy ΔH at a heating rate of 20 K/min. All samples were sealed in Al pans under dry argon gas for the DSC experiments. For the c_p measurements, the DSC was cooled to liquid-nitrogen temperatures. Starting from the lowest temperature, three subsequent scans were made including an empty Al pan of equivalent mass, a sapphire single crystal used as a standard, and of the sample itself (300 mg). By

 0021-8979/90/041744-05$03.00

dividing the temperature range into overlapping intervals of 80 K, the relative error of the c_p measurement was minimized. In comparison with reference samples of unmilled powder, the c_p measurements agreed with literature data to within 2%.[7]

III. EXPERIMENTAL RESULTS

X-ray diffraction data indicate that for the mechanically alloyed Al/Zr powder mixtures, none of the thermodynamically stable intermetallic compounds that appear in the stable phase diagram[8] are formed. Instead, after 12 h of ball milling three different metastable phases are found experimentally, as shown in Fig. 1 as a function of composition of the initial powder mixture: (1) α-Zr (hexagonal structure) supersaturated by Al for x_{Al} less than 0.15 [Fig. 1(a)], (2) a completely amorphous phase for x_{Al} between 0.15 and 0.4 [Fig. 1(b)], and (3) a nanocrystalline ZrAl compound phase with fcc structure for $x_{Al} = 0.5$ [Fig. 1(c)]. For Al concentrations higher than 60 at. %, ball milling does not lead to homogeneous alloy phase formation after extended milling times. For these high Al concentrations, the elemental Al powder does not mix but sinters into large particles of millimeter size making the MA process very inefficient.

By standard metallography methods using SEM, it is found that during the MA process a layered structure of alternating Al and Zr layers is formed. To investigate further the sequence of phase transformations involved in the solid-state amorphization process and the formation of other metastable phases, x-ray diffraction patterns were obtained for the different compositions as a function of ball milling time.

Figure 2 shows a sequence of x-ray diffractograms for $Zr_{0.75}Al_{0.25}$. After 2-h ball milling [see Fig. 2(a)] the (111) Bragg peak related to fcc Al at 38.47° for 2Θ is still detectable. Further processing leads to the disapperance of the (111) Al Bragg peaks, indicating that Al is dissolved completely in Zr after 8 h MA [Fig. 2(b)]. In addition, it is found that the Bragg peaks related to α-Zr are shifted towards higher angles when compared with the Bragg peaks

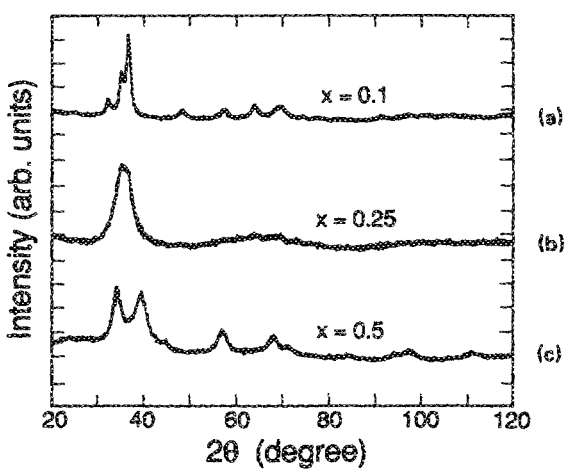

FIG. 1. X-ray diffraction patterns (Cu$K\alpha$ radiation) after 12 h ball milling resulting in (a) supersaturated α-Zr for $x_{Al} \leq 0.15$, (b) an amorphous phase for $0.15 < x_{Al} \leq 0.4$, and (c) a metastable fcc phase for $x_{Al} = 0.5$.

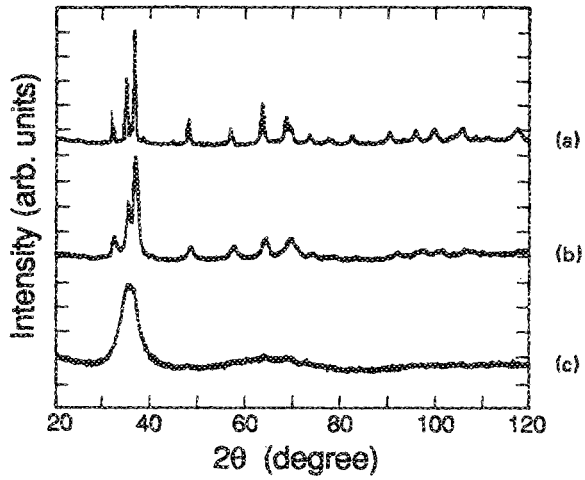

FIG. 2. X-ray diffraction patterns of (Cu$K\alpha$ radiation) of ball-milled powder with initial average composition $Zr_{0.75}Al_{0.25}$ as a function of milling time after (a) 2, (b) 8, and (c) 12 h milling.

of pure Zr. This demonstrates that Al atoms are dissolved in the hexagonal Zr crystal, causing the lattice parameter of α-Zr to shrink. Moreover, during the MA process the α-Zr Bragg peaks become considerably broadened due to the strains that develop and to reduction of the grain size. A simple analysis based on the Scherrer formula indicates that the average grain size decreases from several micrometers in the starting Zr powder to about 12 nm for $Zr_{0.75}Al_{0.25}$ samples after 8 h. After 12-h ball milling the supersaturated Zr crystal becomes unstable and transforms to an amorphous phase, as seen in Fig. 2(c) from the complete disappearance of the Bragg peaks. Transmission electron microscopy analysis supports these findings. TEM bright-field micrographs for $Zr_{0.75}Al_{0.25}$ after 3-h ball milling show considerable strains that develop in the area of shear bands. Further ball milling leads to the amorphization of this sample, as shown in Fig. 3, indicated by the broad halo in the diffraction pattern. This behavior is found for alloy compositions between 17.5 and 40 at. % Al.

For alloy compositions with 15 at. % Al or less, supersaturation of the Zr crystals by aluminum atoms is found as indicated by a maximum lattice parameter change from $a = 3.235$ Å to $a = 3.200$ Å and $c = 5.196$ Å to $c = 5.148$ Å for $Zr_{0.85}Al_{0.15}$ after 12-h ball milling. Further ball milling does not lead to quantitative changes in the microstructure of the powder particles which remain crystalline after 12-h ball milling. The final product of powder mixtures with up to 15 at. % Al is found to be a supersaturated hexagonal nanocrystalline phase with a grain size of approximately 12 nm.

A further increase in Al concentration leads to the synthesis of a metastable crystalline phase not found previously. Again, MA causes the Zr crystals to become destabilized by the incorporation of Al atoms. The transition sequence for $Zr_{0.5}Al_{0.5}$ is as follows: first, α-Zr is supersaturated by Al. Then the sample transforms partially to a glass after 6 h and, finally, the glass crystallizes during further MA to a new metastable phase with fcc structure having a lattice parameter of $a = 4.6093$ Å as revealed by a Nelson–Riley plot analysis.[9] The grain size is estimated from x-ray data to be about 4 nm. This is further supported by TEM results. Figure 4

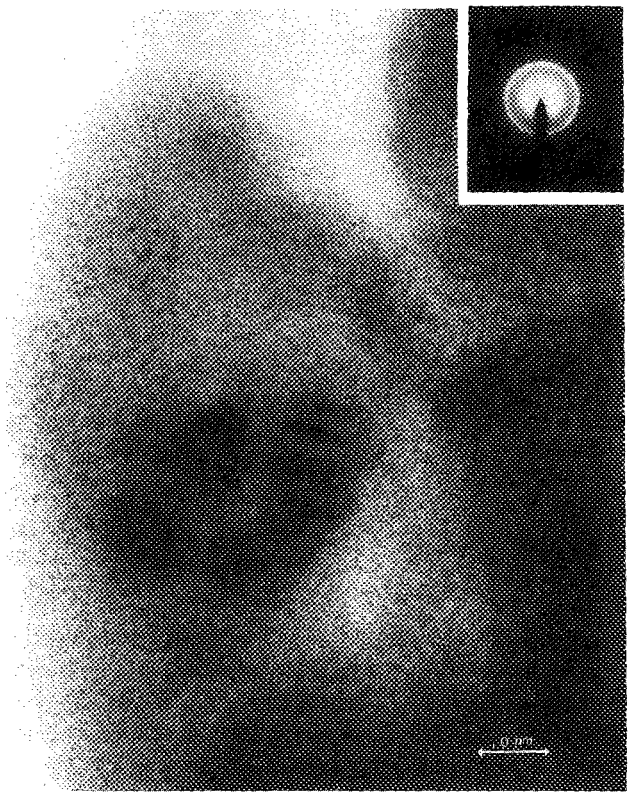

FIG. 3. TEM bright-field image of the amorphous $Zr_{0.75}Al_{0.25}$ phase obtained after 12-h ball milling. The inset shows the corresponding diffraction pattern.

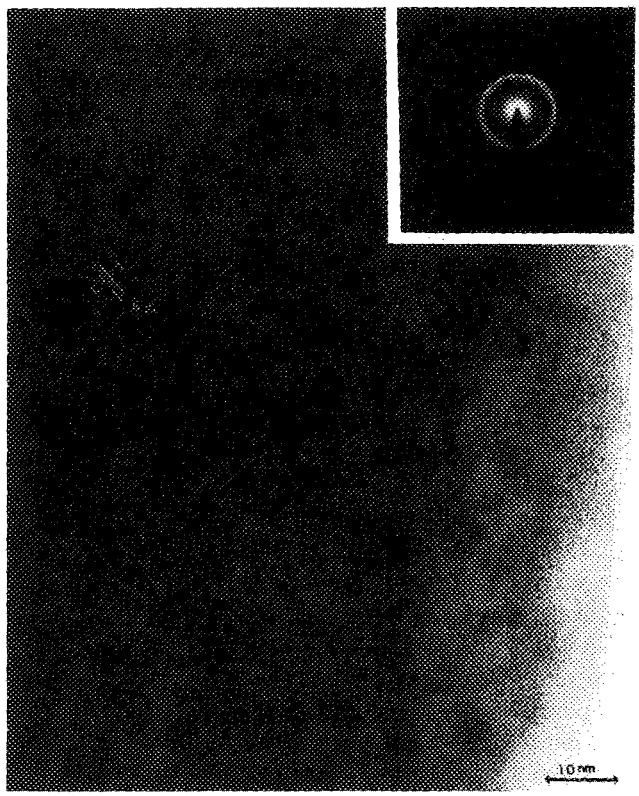

FIG. 4. TEM high-resolution bright-field image for a Zr-Al powder mixture with $x_{Al} = 0.5$ including the corresponding diffraction pattern. The resulting metastable crystalline phase has an fcc structure and an average grain size of 4 nm.

shows a high-resolution micrograph of $Zr_{0.5}Al_{0.5}$ after 12-h ball milling, including the corresponding diffraction pattern. The distance between the lattice fringes if oriented appropriately is found to be about 4 Å, as indicated in Fig. 4. The diffraction pattern and the lattice fringes of the crystals show that the relative orientation of neighboring crystals is completely random. The grain size as estimated from the TEM pictures is found to be 4 nm, in good agreement with the estimation from x-ray peak broadening. This compound cannot be destabilized by further ball milling.

Thermal analysis using DSC allows monitoring of the heat release during crystallization of the amorphous phase. Figure 5 shows a heating scan of an amorphous $Zr_{0.75}Al_{0.25}$ sample indicating crystallization of the glass within a relatively broad temperature range around 720 K. The heat of crystallization corresponds to 4.3 ± 0.5 kJ/mol and is independent of the alloy composition. The crystallization results in a mixture of crystalline compound phases as given in the stable phase diagram.[8] The kinetics of this crystallization reaction can be examined by a Kissinger analysis[10] based on the peak position changes for DSC curves with different scanning rates S (varied between 1 and 20 K/min). By plotting $\ln(S/T^2)$ vs $(1/T)$ the Kissinger analysis yields an activation energy of 2.37 ± 0.05 eV (Fig. 6).

In addition, the specific heat of the ball-milled powder samples has been measured. Figure 7 shows the heat capacity difference Δc_p between the ball-milled samples (after 12 h) and an ideal Zr-Al solid solution at room temperature as a function of alloy concentration. Heat capacity data were measured below 400 K, the temperature at which considerable recovery and recrystallization starts. For pure Zr an increase of 5% in c_p is found. The heat capacity difference between the ball milled powder and an ideal Zr-Al solution increases with higher Al concentration and reaches a maximum of 12% close to the crystal-to-glass transition at 15 at. % Al.

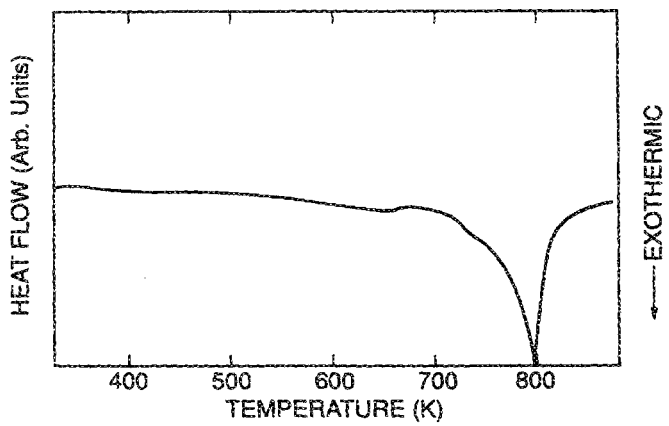

FIG. 5. DSC scan at 20 K/min of a $Zr_{0.75}Al_{0.25}$ powder sample after 12-h ball milling. The exothermic peak corresponds to a heat of crystallization of $\Delta H = 4.3 \pm 0.5$ kJ/mol with a crystallization temperature of about 720 K.

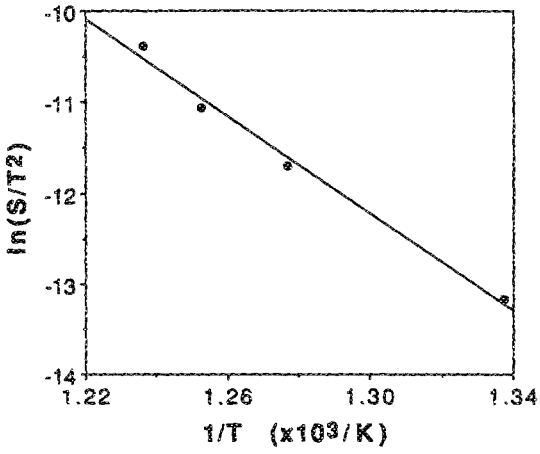

FIG. 6. Plot of $\ln(S/T^2)$ vs $(1/T)$ as obtained from differential calorimetry scans for mechanically alloyed $Zr_{0.75}Al_{0.25}$ at different heating rates S. According to Kissinger's formula an activation energy of $E_a = 2.37$ eV is obtained.

IV. DISCUSSION

By the analysis of x-ray and DSC results for the Zr-Al alloy system, the underlying mechanism of the crystal-to-glass transition can be examined in more detail. As ball milling proceeds, first a layered structure is formed which is refined with increasing processing time. Though the solubility of Al in α-Zr is very small at room temperature for the stable equilibrium with α-Zr, the solubility can be enhanced considerably (up to 15 at. % Al) during nonequilibrium processing like mechanical alloying without formation of the stable compound phases. As indicated by x-ray diffraction, the Al layers dissolve during MA, and Al atoms are incorporated in the α-Zr due to the large negative enthalpy of mixing for Zr-Al.[11] This leads to the development of a concentration profile of Al in Zr and a related lattice parameter change, the average of which has been determined experimentally. For $Zr_{0.85}Al_{0.15}$ samples, the average atomic volume change is found to be about -2% if compared to pure α-Zr and $+2.5\%$ if compared to an ideal solid solution between Zr and Al (linear average atomic volume dependence). For Al concentrations above 15 at. % the hexagonal structure becomes unstable and collapses to a glass. In other words, during MA, the hexagonal α-Zr phase is gradually supersaturated by Al atoms as the MA process proceeds and "melts" to a glass above a certain Al concentration. This chemically induced melting transition has been hypothesized previously on the basis of polymorphous phase diagrams and kinetic constraints imposed on the system as long as the formation of the intermetallic compound phases is kinetically suppressed.[12] In addition, it is interesting to note that the observed change in atomic volume ($+2.5\%$) is about the same as that required for glass formation of ion-bombarded Zr_3Al ($+3\%$)[6] suggesting a similar underlying mechanism (elastic instability.)

Figure 8 shows schematical Gibbs free-energy curves of a binary alloy AB appropriate for the case under consideration. The crystalline phase (e.g. hex-Zr) can lower its free energy by incorporating B atoms up to a certain concentration $C_{B'}$. At this concentration the crystal is in metastable equilibrium with the amorphous phase of composition $C_{B''}$ given by the common tangent construction. Increasing the concentration C_B further, the energy of the crystalline α phase increases and a driving force $\Delta G = \Delta G(C_B)$ develops for formation of the amorphous phase. To nucleate the amorphous phase, a critical nucleus has to be formed having a composition different from that of the crystalline phase. If such compositional fluctuations are prohibited due to the low processing temperature, the solubility can be extended up to a critical value C_B^* where the free energies of the crystalline and amorphous phase become equal. Here the crystal becomes unstable and undergoes a catastrophic transition to a glass.[12] According to our experimental results C_B^* seems to be about 15 at. % Al.

This transition is monitored by the c_p data shown in Fig. 7. The excess heat capacity is a measure of the degree of chemical and topological disorder induced in the crystal lattice. By a drastic reduction of the grain size to about 12 nm and the related incorporation of high-angle grain boundaries

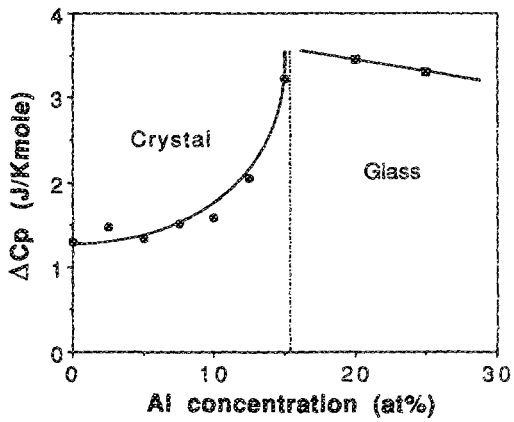

FIG. 7. Excess heat capacity Δc_p in comparison to an ideal Zr-Al solid solution as a function of Al concentrations up to 25 at. %. The data are obtained at 300 K from DSC measurements. The solid line is a guide to the eye.

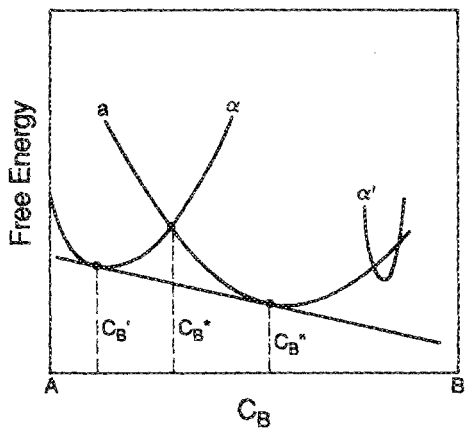

FIG. 8. Schematic free-energy diagram of a binary alloy AB representative of the Zr-Al alloy system, including the solid solution α, the amorphous phase a, and a metastable phase α'.

and related defects, an increase in c_p of 5% is found for pure Zr. Alloying with Al leads to the formation of a metastable disordered solid solution accompanied by an additional increase in anharmonicity of the Zr crystal lattice if compared with the stable ordered compounds. This results in a further increase of c_p, reaching a value of 12% for $x_{Al} = 0.15$ as compared to an ideal solid solution of Al and Zr. The transition of the strongly anharmonic crystal close to the instability cannot be mapped out completely because of the inherent inhomogeneity of the ball milling process. Due to the multilayer formation and diffusional processes during MA, a concentration profile of Al atoms develops in the Zr layers with higher Al concentration at the interface between Al and Zr. Thus, the crystal-to-glass transition becomes localized close to the layer interfaces in the early stage of the transformation. During further ball milling the amorphous phase will grow at the expense of the remaining crystalline phase. Therefore, if one is close to the instability only the average of the heat capacity of the crystalline and amorphous phase can be determined.

The excess enthalpy that is stored in the glass as compared to that of the stable compound phases is 4.3 ± 0.5 kJ/mol, corresponding to approximately 30% of the enthalpy of fusion ΔH_f of the compound phases. It is interesting to note that a major portion of this energy (20% ΔH_f) can be stored by the incorporation of lattice defects like grain boundaries and dislocations resulting from ball milling, as found for pure Zr powder samples.[13] Because pure metals exhibit a strong resistance against vitrification, an amorphous phase based on a pure metal has not been found above cryogenic temperatures. Thus, to form a metallic glass it is necessary to include chemical disorder in the Zr crystal, which can be achieved by alloying with a number of elements having a negative heat of mixing with Zr, like Ni, Al, Fe, etc. The additional chemical energy resulting from the chemical disorder induced by MA then drives the system to the amorphous state. Because the mechanical alloying and deformation process proceeds at relatively low temperatures (if compared to the melting point) the recovery rate for the topological and chemical disorder introduced into the crystal is low. Actually, for Zr alloys the effective local temperature in the powder particles at the collision site has been determined to be about 150 K above room temperature.[14] Hence, by alloying with 15 at. % Al, the melting point of α-Zr—which is metastable at high temperature with respect to the bcc phase—is reduced from 1820 K, as estimated by Kaufmann,[15] to approximately room temperature. This leads to vitrification of the crystalline phase at the prevalent milling conditions due to the statical disorder built into the Zr lattice.

V. CONCLUSIONS

Although it is not probable that the entire sample transforms simultaneously to the amorphous phase due to fluctuations in the local Al concentration, the x-ray results, specific heat behavior, and thermodynamic arguments strongly suggest that the amorphization process of α-Zr observed here can be viewed as a compositionally induced melting transition when the crystal is driven outside of its own stability range. The melting temperature of α-Zr has been reduced from 1820 K to about room temperature by increasing the Al concentration and introducing structural defects (such as point defects, dislocations, and grain boundaries) into the crystalline lattice during mechanical alloying. For the $Zr_{0.75}Al_{0.25}$ amorphous sample produced under the given conditions, the crystallization reaction starts at about 720 K with an enthalpy of crystallization of $\Delta H = 4.3 \pm 0.5$ kJ/mol. A nanocrystalline supersaturated solid solution of α-Zr for $x_{Al} \leqslant 0.15$ and a metastable fcc phase of ZrAl can also be prepared by the MA process.

ACKNOWLEDGMENTS

The financial support by the U.S. Department of Energy (DOE Contract No. DE-FG03-86ER45242) is gratefully acknowledged. The authors are indebted to C. Garland for the TEM work and E. Hellstern, Y. Seki, and C. E. Krill III for useful discussions.

[1] W. L. Johnson, Prog. Mater. Sci. **30**, 81 (1986).
[2] A. Y. Yermakov, Y. Y. Yurchikov, and V. A. Barinov, Phys. Met. Metallogr. **52**, 50 (1981).
[3] R. B. Schwarz, R. R. Petrich, and C. K. Saw, J. Non-Cryst. Solids **76**, 281 (1985).
[4] E. Hellstern and L. Schultz, Appl. Phys. Lett. **48**, 124 (1986).
[5] C. C. Koch, O. B. Cavin, C. G. McKamey, and J. O. Scarborough, Appl. Phys. Lett. **43**, 1017 (1983).
[6] L. E. Rehn, P. R. Okamoto, J. Pearson, R. Bhadra, and M. Grimsditch, Phys. Rev. Lett. **59**, 2987 (1987).
[7] R. Hultgren, P. D. Desai, D. T. Hawkins, M. Gleiser, K. K. Kelley, and D. D. Wagman, *Selected Values of the Thermodynamic Properties of the Elements* (American Society of Metals, Metals Park, OH, 1973).
[8] T. B. Massalski, *Binary Alloy Phase Diagrams* (American Society of Metals, Metals Park, OH, 1986).
[9] J. B. Nelson and D. P. Riley, Proc. Phys. Soc. London **57**, 160 (1945).
[10] H. E. Kissinger, Anal. Chem. **29**, 1702 (1957).
[11] A. K. Niessen, F. R. de Boer, R. Boom, P. F. de Chatel, W. C. M. Mattens, and A. R. Miedema, CALPHAD **7**, 51 (1983).
[12] H. J. Fecht and W. L. Johnson, Nature **334**, 50 (1988).
[13] H. J. Fecht, E. Hellstern, Z. Fu, and W. L. Johnson, Metall. Trans. (in press).
[14] R. Schulz, M. Trudeau, J. Y. Huot, and A. Van Neste, Phys. Rev. Lett. **62**, 2849 (1989).
[15] L. Kaufmann and H. Bernstein, *Computer Calculation of Phase Diagrams* (Academic, New York, 1970).